Combustion Theory and Modelling
Vol. 14, No. 2, 2010, 177–202

Triple-flame propagation in a parallel flow: an analytical study

Joel Daou[a*] and Faisal Al-Malki[b]

[a]*School of Mathematics, University of Manchester, Manchester M13 9PL, UK;*
[b]*Department of Mathematics, Taif University, Taif P.O.Box 888, Saudi Arabia*

(*Received 16 December 2009; final version received 15 February 2010*)

We present an analytical study of triple-flame propagation in a two-dimensional mixing layer against a parallel flow. The problem is formulated within a constant density thermo-diffusive model, and solved analytically in the asymptotic limit of large activation energy of the chemical reaction for flames thin compared with their typical radius of curvature. Explicit expressions are obtained in this limit, describing the influence of the flow on the triple-flame. The results are expected to be applicable when the ratio between the flow-scale and the flame-front radius of curvature (which is mainly dictated by concentration gradients) is of order unity, or larger. When this ratio is large, as in the illustrative case of a Poiseuille flow in a porous channel considered here, the flow is found to negligibly affect the flame structure except for a change in its speed by an amount which depends on the stoichiometric conditions of the mixture. On the other hand, when this ratio is of order unity, the flow is able to significantly wrinkle the flame-front, modify its propagation speed, and shift its leading edge away from the stoichiometric line. The latter situation is investigated in the illustrative case of spatially harmonic flows. The results presented describe, in particular, how the leading-edge of the flame-front can be determined in terms of the flow amplitude A which is critical in determining the flame speed. The latter is found to depend linearly on A in the first approximation with a correction proportional to the flame thickness multiplied by $\sqrt{|A|}$, for $|A|$ sufficiently large. The effect of varying the flow-scale on flame propagation in this context is also described, with explicit formulae provided, and interesting behaviours, such as non-monotonic dependence on the scale, identified.

Keywords: triple-flames; flame-flow interaction; partially premixed flames

1. Introduction

Flame propagation in a flow field is an important problem from both theoretical and practical points of view, characterized in general by the interaction of a curved flame with a flow that can involve a wide range of temporal and spatial scales. The problem is often further complicated by the presence of various inhomogeneities in the combustion mixture itself. These include the spatial non-uniformities in the composition of the reactants and their temperature, which are frequently encountered in non-premixed combustion situations such as in a mixing layer of initially non-premixed reactants. Typically, the composition of the reactive mixture varies across the mixing layer from fuel-lean to fuel-rich, which leads to the formation of triple-flames. Such flames, consisting of two premixed branches and a trailing diffusion flame, were first observed experimentally by Philips in 1965 [1]. Early analytical

*Corresponding author. Email: joel.daou@manchester.ac.uk

ISSN: 1364-7830 print / 1741-3559 online

DOI: 10.1080/13647831003713948
http://www.informaworld.com

investigation of these structures was carried out by Ohki and Tsuge [2]. More detailed analyses were then undertaken by Dold [3] and Dold and Hartley [4], who examined the dependence of the shape and the propagation speed of triple-flames on the transverse mixture gradient through which they propagate. Over the past 20 years, a large number of studies have been devoted to triple-flames due to their importance in applications involving combustion phenomena such as flame propagation in mixing layers, flame spread over solid fuel surfaces, and autoignition fronts in diesel engines [5]. Many aspects of triple-flames have been to date investigated theoretically or experimentally including preferential diffusion [6], heat losses [7–9], reversibility of the chemical reaction [10, 11] and other factors [9, 12, 13].

The purpose of the present work is to study the response of triple-flames to the presence of a flow field, in the simple situation where the flow is in the direction of flame propagation. The study, which seems to have received no attention in the literature, can be viewed as a first step towards understanding the important problem of the propagation of partially premixed flames in turbulent flows. As a framework for the investigation we consider a thermo-diffusive model representing a steady single-scale parallel flow along an unstrained mixing layer where the reactants – fuel and oxidizer – diffuse into each other to support a propagating triple-flame. The corresponding problem is tackled analytically using an asymptotic approach under suitably defined conditions. The main aim is to assess the effect of the flow on the structure and propagation speed of the triple-flame.

The paper is organized as follows. We begin by describing the thermo-diffusive model adopted and formulating the corresponding problem in Section 2. This is followed by an asymptotic analysis which is based on a compact reformulation of the problem derived in Section 3 in the limit of infinitely large activation energy of the chemical reaction. The reformulated problem is solved analytically for flame-fronts thin compared with their typical radius of curvature (which is mainly dictated by concentration gradients) in Section 4. The analytical solution obtained results in explicit expressions, describing the influence of the flow on the triple-flame, which are expected to be applicable when the ratio between the flow-scale and the flame-front radius of curvature is of order unity, or larger. Section 5 addresses the case when this ratio is large in the illustrative example of a Poiseuille flow in a porous channel. Then, in Section 6 we study the situation when this ratio is of order one within the illustrative case of spatially harmonic flows. Finally, a summary of the main results and recommendations for further work close the paper.

2. Formulation

We consider triple-flame propagation in a channel of width $2L$ against a parallel flow moving along the X-direction, as shown in Figure 1. The walls of the channel are assumed

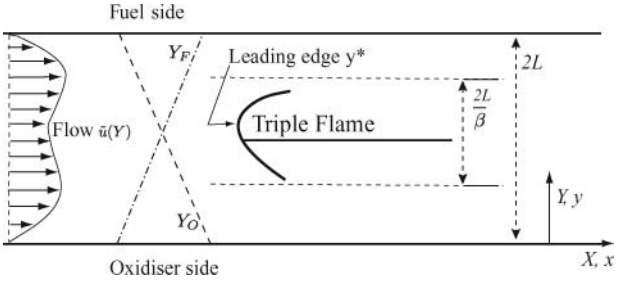

Figure 1. A schematic illustration of triple-flame propagation against a parallel flow $\tilde{u}(Y)$. The mass fractions are prescribed by $Y_F = Y_{F,F}$ and $Y_O = 0$ on the fuel side, and $Y_F = 0$ and $Y_O = Y_{O,O}$ on the oxidizer side.

to be porous and that the concentrations of fuel and oxidizer are maintained fixed at the walls. Although such a setup may be difficult to achieve experimentally, it is adopted here as a simple theoretical model to understand the effect of a flow on the triple-flame. The combustion is represented by a single irreversible one-step reaction of the form

$$\mathrm{F} + s\mathrm{O} \rightarrow (1+s)\mathrm{P} + q,$$

where F denotes the fuel, O the oxidizer and P the products. The quantity s denotes the mass of oxidizer consumed and q the heat released, both per unit mass of fuel. We consider a thermo-diffusive approximation with constant density and constant transport properties. The governing equations in dimensional form can be written

$$(\tilde{V} + \tilde{u}(Y))\frac{\partial T}{\partial X} = D_{\mathrm{T}}\left(\frac{\partial^2 T}{\partial X^2} + \frac{\partial^2 T}{\partial Y^2}\right) + \frac{q}{c_p}\frac{\tilde{\omega}}{\rho} \tag{1}$$

$$(\tilde{V} + \tilde{u}(Y))\frac{\partial Y_{\mathrm{F}}}{\partial X} = D_{\mathrm{F}}\left(\frac{\partial^2 Y_{\mathrm{F}}}{\partial X^2} + \frac{\partial^2 Y_{\mathrm{F}}}{\partial Y^2}\right) - \frac{\tilde{\omega}}{\rho} \tag{2}$$

$$(\tilde{V} + \tilde{u}(Y))\frac{\partial Y_{\mathrm{O}}}{\partial X} = D_{\mathrm{O}}\left(\frac{\partial^2 Y_{\mathrm{O}}}{\partial X^2} + \frac{\partial^2 Y_{\mathrm{O}}}{\partial Y^2}\right) - s\frac{\tilde{\omega}}{\rho}. \tag{3}$$

These equations are written *in a frame of reference attached to the flame whose propagation speed relative to the laboratory is* $\tilde{V}$*, with* $\tilde{V} > 0$ *indicating a propagation to the left*. The velocity of the parallel flow along the positive X-direction relative to the laboratory is denoted by $\tilde{u}(Y)$. The flame speed $\tilde{V}$ is an eigenvalue of the problem and must be determined as part of the solution. Here T, Y_{F} and Y_{O} are respectively the temperature and the mass fraction of the fuel and oxidizer. In addition, D_{F}, D_{O}, and D_{T} denote the diffusion coefficients of the fuel, the oxidizer, and heat respectively, and are taken to be constants. The quantities ρ and c_p denote the density and the heat capacity. The reaction rate $\tilde{\omega}$, defined as the mass of fuel consumed per unit volume and unit time, obeys an Arrhenius law

$$\tilde{\omega} = B\rho^2 Y_{\mathrm{F}} Y_{\mathrm{O}} \exp(-E/RT), \tag{4}$$

where B and E/R represent, respectively, the (constant) pre-exponential factor and the activation temperature.

The conditions as $X \rightarrow -\infty$ correspond to the frozen solution independent of X, which is given by

$$T = T_{\mathrm{u}} \tag{5a}$$

$$Y_{\mathrm{F}} = \frac{Y_{\mathrm{F,F}}}{2}\left(1 + \frac{Y}{L}\right) \tag{5b}$$

$$Y_{\mathrm{O}} = \frac{Y_{\mathrm{O,O}}}{2}\left(1 - \frac{Y}{L}\right), \tag{5c}$$

where $Y_{\mathrm{F,F}}$ and $Y_{\mathrm{O,O}}$ refer to the mass fraction of the fuel side and the oxidizer side respectively, and T_{u} refers to the temperature on both sides as well as in the unburnt mixture; thus, the lateral boundary conditions are also given by (5) with $Y \rightarrow \pm L$ for all X.

Downstream, at $X \to \infty$, the solution again becomes independent of X, corresponding to the one-dimensional strongly burning solution of the diffusion flame.

For large activation energies, the flame-front region is expected to be centred around the stoichiometric surface. Upstream, this surface is located at $Y = Y_{\rm st}$ where $Y_{\rm st}$ is determined from $Y_{\rm O} = sY_{\rm F}$ and Equations (5) to be

$$\frac{Y_{\rm st}}{L} = \frac{1-S}{1+S}, \tag{6}$$

where $S \equiv sY_{\rm F,F}/Y_{\rm O,O}$ is a normalized stoichiometric coefficient.

Next, we write the governing equations in terms of the scaled quantities

$$y_{\rm F} = \frac{Y_{\rm F}}{Y_{\rm F,st}}, \qquad y_{\rm O} = \frac{Y_{\rm O}}{Y_{\rm O,st}}, \qquad \theta = \frac{T-T_{\rm u}}{T_{\rm ad}-T_{\rm u}}, \tag{7}$$

where the subscript 'st' indicates values at $(X \to -\infty, Y = Y_{\rm st})$ and where $T_{\rm ad} \equiv T_{\rm u} + qY_{\rm F,st}/c_p$ is the adiabatic flame temperature.

To non-dimensionalize the problem, we follow [6] and select as **unit length** L/β, (half) the ratio between the mixing layer thickness and the Zeldovich number $\beta \equiv E(T_{\rm ad} - T_{\rm u})/RT_{\rm ad}^2$, which represents the typical radius of curvature of the triple-flame. As **unit speed** we select the laminar speed of the stoichiometric planar flame $S_{\rm L}^0$, which for large β is given by

$$S_{\rm L}^0 = \sqrt{\frac{4{\rm Le_F Le_O}}{\beta^3} Y_{\rm O,st}(\rho D_{\rm T})B \exp\left(\frac{-E}{RT_{\rm ad}}\right)}. \tag{8}$$

Substituting 7 into Equations (1–3) leads to the non-dimensional model

$$(V+u(y))\frac{\partial\theta}{\partial x} = \epsilon\left(\frac{\partial^2\theta}{\partial x^2} + \frac{\partial^2\theta}{\partial y^2}\right) + \epsilon^{-1}\omega \tag{9}$$

$$(V+u(y))\frac{\partial y_{\rm F}}{\partial x} = \frac{\epsilon}{{\rm Le_F}}\left(\frac{\partial^2 y_{\rm F}}{\partial x^2} + \frac{\partial^2 y_{\rm F}}{\partial y^2}\right) - \epsilon^{-1}\omega \tag{10}$$

$$(V+u(y))\frac{\partial y_{\rm O}}{\partial x} = \frac{\epsilon}{{\rm Le_O}}\left(\frac{\partial^2 y_{\rm O}}{\partial x^2} + \frac{\partial^2 y_{\rm O}}{\partial y^2}\right) - \epsilon^{-1}\omega, \tag{11}$$

in terms of the coordinates $x = \beta X/L$ and $y = \beta(Y - Y_{\rm st})/L$. Here

$$\epsilon \equiv \frac{\ell_{\rm Fl}}{L/\beta} = \frac{D_{\rm T}/S_{\rm L}^0}{L/\beta}, \tag{12}$$

represents the thickness of the laminar stoichiometric flame $\ell_{\rm Fl} \equiv D_{\rm T}/S_{\rm L}^0$ measured in terms of the reference length L/β. The non-dimensional reaction rate ω is given by

$$\omega = \frac{\beta^3}{4{\rm Le_F Le_O}} y_{\rm F} y_{\rm O} \exp\left(\frac{\beta(\theta-1)}{1+\alpha(\theta-1)}\right), \tag{13}$$

where $\alpha = (T_{\rm ad} - T_{\rm u})/T_{\rm ad}$. Finally, V and $u(y)$ are the non-dimensional propagation speed and flow velocity (both relative to the laboratory).

The upstream and lateral boundary conditions are

$$\theta = 0 \tag{14a}$$

$$y_{\mathrm{F}} = 1 + \gamma_{\mathrm{F}} \frac{y}{\beta} \tag{14b}$$

$$y_{\mathrm{O}} = 1 - \gamma_{\mathrm{O}} \frac{y}{\beta}, \qquad \text{as} \quad x \to -\infty,\ y \to \frac{\beta}{\gamma_{\mathrm{O}}} \ \text{or}\ y \to -\frac{\beta}{\gamma_{\mathrm{F}}}, \tag{14c}$$

where

$$\gamma_{\mathrm{F}} = \frac{1+S}{2} \qquad \text{and} \qquad \gamma_{\mathrm{O}} = \frac{1+S}{2S}. \tag{15}$$

Downstream, we require that

$$\frac{\partial y_{\mathrm{F}}}{\partial x} = \frac{\partial y_{\mathrm{O}}}{\partial x} = \frac{\partial \theta}{\partial x} = 0 \qquad \text{as } x \to \infty. \tag{16}$$

The problem now is fully formulated by Equations (9–11) with the boundary conditions (14–16). The solution of this problem, e.g. numerically, can provide, in addition to the profiles of θ, y_{F}, and y_{O}, the flame speed V in terms of $u(y)$, Le_{F}, Le_{O}, S , ϵ, β and α. For the sake of an analytical treatment, however, we consider herein the problem in the limiting case $\beta \to \infty$ where a compact reformulation can be derived, and solved analytically when the radius of curvature is large compared with the flame thickness (i.e. for $\epsilon \ll 1$). The derivation of this reformulation is given next.

3. The large activation energy asymptotic limit

3.1. *A β-free reformulated problem*

In this section, we derive a compact formulation valid in the distinguished limit $\beta \to \infty$ with $\epsilon = \mathcal{O}(1)$. The analysis is restricted to near equidiffusion flames for which

$$\mathrm{Le}_{\mathrm{F}} \sim 1 + \frac{l_{\mathrm{F}}}{\beta} \qquad \text{and} \qquad \mathrm{Le}_{\mathrm{O}} \sim 1 + \frac{l_{\mathrm{O}}}{\beta},$$

where l_{F} and l_{O} are the reduced Lewis numbers of the fuel and oxidizer respectively. In this limit, the reaction zone is confined to an infinitely thin sheet that we shall call the flame surface, which is given by $F(x, y) = x - f(y) = 0$, say. A reformulation of the problem free from the presence of β can then be derived as in [6]. Consider a coordinate system attached to the flame

$$\xi = x - f(y), \qquad y = y,$$

so that the flame surface is located at $\xi = 0$. Expand the dependent variables in terms of β^{-1} in the form

$$\theta = \theta^0 + \frac{\theta^1}{\beta} + \cdots, \quad y_{\mathrm{F}} = y_{\mathrm{F}}^0 + \frac{y_{\mathrm{F}}^1}{\beta} + \cdots, \quad y_{\mathrm{O}} = y_{\mathrm{O}}^0 + \frac{y_{\mathrm{O}}^1}{\beta} + \cdots$$

In the reaction zone and behind it, we assume that $\theta^0 = 1$ and $y_F^0 = y_O^0 = 0$, which leads to

$$\theta = 1 + \frac{\theta^1}{\beta} + \cdots, \quad y_F = \frac{y_F^1}{\beta} + \cdots, \quad y_O = \frac{y_O^1}{\beta} + \cdots, \quad \text{for } \xi \geq 0. \tag{17}$$

The reaction term can be eliminated from Equations (9–11) by using the variables $Z_F \equiv \theta + y_F$ and $Z_O \equiv \theta + y_O$ which when substituted into (9–11) leads to

$$(V + u(y))\frac{\partial Z_F}{\partial \xi} = \epsilon \Delta Z_F - \epsilon \frac{l_F}{\beta} \Delta y_F, \tag{18}$$

$$(V + u(y))\frac{\partial Z_O}{\partial \xi} = \epsilon \Delta Z_O - \epsilon \frac{l_O}{\beta} \Delta y_O, \tag{19}$$

where $u(y)$ represents the flow in the limit $\beta \to \infty$ and $y = \mathcal{O}(1)$. The variables Z_F and Z_O can be expanded as

$$Z_F = Z_F^0 + \frac{Z_F^1}{\beta} + \cdots, \qquad Z_O = Z_O^0 + \frac{Z_O^1}{\beta} + \cdots, \tag{20}$$

but since $\theta^0 + y_F^0 = 1$ and $\theta^0 + y_O^0 = 1$ everywhere, one obtains

$$Z_F^0 = \theta^0 + y_F^0 = 1\,, \qquad Z_F^1 = \theta^1 + y_F^1 \equiv h(\xi, y)\,,$$
$$Z_O^0 = \theta^0 + y_O^0 = 1\,, \qquad Z_O^1 = \theta^1 + y_O^1 \equiv k(\xi, y)\,.$$

Substitution of (17) and (20) into Equations (9), (18) and (19) yield the governing equations for θ^0, h and k in the form

$$(V + u(y))\frac{\partial \theta^0}{\partial \xi} = \epsilon \Delta \theta^0, \tag{21}$$

$$(V + u(y))\frac{\partial h}{\partial \xi} = \epsilon \Delta h + \epsilon l_F \Delta \theta^0, \tag{22}$$

$$(V + u(y))\frac{\partial k}{\partial \xi} = \epsilon \Delta k + \epsilon l_O \Delta \theta^0, \tag{23}$$

which are to be solved on both sides of the reaction sheet where $\xi \neq 0$, with the upstream boundary conditions

$$\theta^0 = 0, \qquad h = \gamma_F y, \qquad k = -\gamma_O y \qquad \text{as} \quad \xi \to -\infty \tag{24}$$

and the downstream boundary conditions

$$\frac{\partial \theta^0}{\partial \xi} = \frac{\partial h}{\partial \xi} = \frac{\partial k}{\partial \xi} = 0 \qquad \text{as} \quad \xi \to \infty\,. \tag{25}$$

The jump conditions at $\xi = 0$ are

$$[\theta^0] = [h] = [k] = 0\,, \tag{26a}$$

$$\left[\frac{\partial h}{\partial \xi}\right] = -l_{\mathrm{F}}\left[\frac{\partial \theta^0}{\partial \xi}\right], \qquad \left[\frac{\partial k}{\partial \xi}\right] = -l_{\mathrm{O}}\left[\frac{\partial \theta^0}{\partial \xi}\right], \tag{26b}$$

$$\epsilon\sqrt{1+f'^2}\left[\frac{\partial \theta^0}{\partial \xi}\right] = -\sqrt{1+\frac{|h-k|}{2}}\exp\left(\frac{h+k-|h-k|}{4}\right), \tag{26c}$$

which can be derived following the methodology described in [11]; see also [14, p. 39].

3.2. *Leading edge of the flame-front*

A quantity of great interest to our study is *the local burning speed* S_{L}, which is defined as the component of the fluid velocity ahead of the flame-front normal to the flame surface, given by $S_{\mathrm{L}} = \big(V + u(y)\big)\mathbf{i}.\mathbf{n}$, i.e.

$$S_{\mathrm{L}} = \frac{V + u(y)}{(1 + f'(y)^2)^{1/2}}\,. \tag{27}$$

Here, $\mathbf{i}$ and $\mathbf{j}$ are unit vectors in the x and y directions, respectively, and $\mathbf{n} = (\mathbf{i} - f'(y)\mathbf{j})/(1 + f'(y)^2)^{1/2}$ is a unit vector normal to the reaction sheet pointing to the burnt gas.

We now derive a useful criterion for the determination of the leading edge(s) of a flame-front propagating in a parallel flow field, whose local burning speed is given by 27; such a determination is a key step in describing the flame-front of triple-flames, see Figure 1.

Geometrically, a flame-edge, located at $y = y^*$ say, corresponds to a minimum of the function $x = f(y)$, typically characterized by

$$f'(y^*) = 0 \quad \text{and} \quad f''(y^*) > 0\,. \tag{28}$$

It is easy to show that the local flame speed in the negative x-direction with respect to the laboratory given by $S_{\mathrm{L}}(y) - u(y)$ must have a maximum at $y = y^*$. In other words, we must (typically) have

$$S'_{\mathrm{L}}(y^*) - u'(y^*) = 0 \quad \text{and} \quad S''_{\mathrm{L}}(y^*) - u''(y^*) < 0\,. \tag{29}$$

This can be explained by a Taylor expansion of 27 which implies that, for y sufficiently close to a point y^* where $f' = 0$, we have

$$(S_{\mathrm{L}}(y^*) - u(y^*) - V) + (y - y^*)(S'_{\mathrm{L}}(y^*) - u'(y^*)) + \frac{(y-y^*)^2}{2}(S''_{\mathrm{L}}(y^*) - u''(y^*) + S_{\mathrm{L}}(y^*)f''^2(y^*)) + \cdots = 0\,.$$

This expansion implies that

$$V = S_{\mathrm{L}}(y^*) - u(y^*)\,, \tag{30}$$

a formula for the determination of the flame speed V, along with

$$S'_{\mathrm{L}}(y^*) - u'(y^*) = 0 \quad \text{and} \quad S''_{\mathrm{L}}(y^*) - u''(y^*) = -S_{\mathrm{L}}(y^*)f''^2(y^*) < 0, \tag{31}$$

which justifies that $S_L(y) - u(y)$ must have a (local) maximum at $y = y^*$ (unless $f''(y^*)$ or $S_L(y^*)$ vanish).

In fact, under the assumption that $S_L(y)$ is always positive, as it is in the asymptotic study for $\epsilon \ll 1$ carried out below, we may affirm that the *location of a leading edge must correspond to a* **global** *maximum of* $S_L - u$. This statement follows at once from (27) which implies, when used with the fact that $1 + f_y^2 \geq 1$ and $S_L > 0$, that $S_L(y) - u(y) \leq V = S_L(y^*) - u(y^*)$ for any y.

Clearly, there are two factors influencing the location of the leading edge, namely the local burning speed S_L and the flow itself. In the absence of flow, i.e. when $u \equiv 0$, the leading edge corresponds to the location where S_L is maximum according to (29), which is the criterion used in previous studies such as [3, 6, 11] to determine the leading edge. In the presence of the flow, however, the leading edge is determined by a balance between the local burning speed and the flow. Finally, if we introduce the propagation speed

$$U \equiv V + u(y^*)\,, \tag{32}$$

which represents the flame speed with respect to the gas located at $y = y^*$, then (30) shows that $U = S_L(y^*)$, i.e. that U is equal to the burning velocity at the leading edge. We note that the sign of U determines whether the flame-front is an ignition front ($U > 0$) or an extinction front ($U < 0$); however extinctions fronts will not be encountered in the asymptotic analysis below since S_L remains positive in the limit $\epsilon \to 0$, as mentioned above and as will be confirmed shortly.[1]

4. Analytical results in the limit $\epsilon \to 0$

We now consider the limit $\epsilon \to 0$ applied to the β-free reformulated problem of Section 3.1. The results to be derived are expected to be valid provided the activation energy is large and ϵ small, more precisely for $\beta^{-1} \ll \epsilon \ll 1$.

For $\epsilon \to 0$, the flame including its preheat zone can be seen as an infinitely thin layer, located at $\xi = 0$, with thickness of order $\mathcal{O}(\epsilon)$. We introduce expansions in terms of ϵ in the form

$$f(y) = f_0(y) + \epsilon f_1(y) + \cdots, \qquad V = V_0 + \epsilon V_1 + \cdots,$$

with similar expansions for other variables. In particular, for S_L defined in (27) we can write

$$S_L = S_{L0} + \epsilon S_{L1} + \cdots, \tag{33}$$

where

$$S_{L0} = \frac{V_0 + u(y)}{\sqrt{1 + f_0'^2}}, \tag{34}$$

$$S_{L1} = \frac{1}{\sqrt{1 + f_0'^2}} \left[V_1 - \big(V_0 + u(y)\big) \frac{f_0' f_1'}{1 + f_0'^2} \right]. \tag{35}$$

[1] See e.g. Equation 45.

4.1. *Outer solution*

On both sides of the flame ($\xi \neq 0$), we seek expansions in the form

$$\theta^0 = \Theta_0 + \epsilon\Theta_1 + \cdots, \qquad h = H_0 + \epsilon H_1 + \cdots, \qquad k = K_0 + \epsilon K_1 + \cdots,$$

which we substitute into Equations (21–26a). We get to leading order

$$(V_0 + u(y))\frac{\partial \Theta_0}{\partial \xi} = (V_0 + u(y))\frac{\partial H_0}{\partial \xi} = (V_0 + u(y))\frac{\partial K_0}{\partial \xi} = 0,$$

subject to the boundary conditions

$$\begin{aligned} &\Theta_0 = 0, \qquad H_0 = \gamma_{\mathrm{F}} y, \qquad K_0 = -\gamma_{\mathrm{O}} y \quad \text{as} \quad \xi \to -\infty, \\ &\frac{\partial \Theta_0}{\partial \xi} = \frac{\partial H_0}{\partial \xi} = \frac{\partial K_0}{\partial \xi} = 0 \qquad\qquad\qquad\quad \text{as} \quad \xi \to \infty. \end{aligned}$$

We thus find that

$$\Theta_0 = \begin{cases} 0 \\ 1, \end{cases} \qquad H_0 = \begin{cases} \gamma_{\mathrm{F}} y \\ B(y), \end{cases} \qquad K_0 = \begin{cases} -\gamma_{\mathrm{O}} y & (\xi < 0) \\ C(y) & (\xi > 0), \end{cases} \tag{36}$$

where we have used the fact that $\theta^0 = 1$ for $\xi \geq 0$ and where $B(y)$ and $C(y)$ are functions of y which can be determined by matching with the inner solution. We note that $\theta^0 = \Theta_0$ is in fact an outer solution to all orders in ϵ, i.e. that $\Theta_1 = \Theta_2 = \cdots = 0$.

4.2. *Inner solution*

Using the stretched variable $\zeta = \xi/\epsilon$, we write inner expansions in the form

$$\theta^0 = \theta_0 + \epsilon\theta_1 + \cdots, \qquad h = h_0 + \epsilon h_1 + \cdots, \qquad k = k_0 + \epsilon k_1 + \cdots$$

Substituting these in the jump conditions (26a–26c) gives to leading order

$$[\theta_0] = [h_0] = [k_0] = 0, \tag{37a}$$

$$\left[\frac{\partial h_0}{\partial \zeta}\right] = -l_{\mathrm{F}}\left[\frac{\partial \theta_0}{\partial \zeta}\right], \qquad \left[\frac{\partial k_0}{\partial \zeta}\right] = -l_{\mathrm{O}}\left[\frac{\partial \theta_0}{\partial \zeta}\right], \tag{37b}$$

$$\sqrt{1 + f_0'^2}\left[\frac{\partial \theta_0}{\partial \zeta}\right] = -\sqrt{1 + \frac{|h_0 - k_0|}{2}}\exp\left(\frac{h_0 + k_0 - |h_0 - k_0|}{4}\right). \tag{37c}$$

In terms of ζ, the leading order equations in the inner region take the form

$$\frac{\partial^2 \theta_0}{\partial \zeta^2} = \lambda\frac{\partial \theta_0}{\partial \zeta}, \tag{38}$$

$$\frac{\partial^2 h_0}{\partial \zeta^2} = \lambda\frac{\partial h_0}{\partial \zeta} - l_{\mathrm{F}}\frac{\partial^2 \theta_0}{\partial \zeta^2}, \tag{39}$$

$$\frac{\partial^2 k_0}{\partial \zeta^2} = \lambda \frac{\partial k_0}{\partial \zeta} - l_{\mathrm{O}} \frac{\partial^2 \theta_0}{\partial \zeta^2} \tag{40}$$

where

$$\lambda = \frac{V_0 + u(y)}{1 + f_0'^2(y)}. \tag{41}$$

The solution of (38–40) subject to the jump conditions (37a–37b) and the matching requirements with the outer solution (36) can be written as

$$\theta_0 = \begin{cases} \exp(\lambda\zeta) & \zeta < 0 \\ 1 & \zeta > 0 \end{cases} \tag{42}$$

$$h_0 = \begin{cases} \gamma_{\mathrm{F}} y - l_{\mathrm{F}} \lambda\zeta \exp(\lambda\zeta) & \zeta < 0 \\ \gamma_{\mathrm{F}} y & \zeta > 0 \end{cases} \tag{43}$$

$$k_0 = \begin{cases} -\gamma_{\mathrm{O}} y - l_{\mathrm{O}} \lambda\zeta \exp(\lambda\zeta) & \zeta < 0 \\ -\gamma_{\mathrm{O}} y & \zeta > 0, \end{cases} \tag{44}$$

which gives the leading order approximation to the inner solution. We note parenthetically that the matching also determines the constants $B(y)$ and $C(y)$ in 36 as being equal to $\gamma_{\mathrm{F}} y$ and $-\gamma_{\mathrm{O}} y$, respectively.

4.3. *Local burning speed (to leading order)*

At this stage, the local burning speed to leading order S_{L0} given by (34) can be obtained by using the jump condition (37c) together with (43) and (44), whence

$$S_{\mathrm{L0}} = \sqrt{1 + \frac{(\gamma_{\mathrm{F}} + \gamma_{\mathrm{O}})}{2}|y|}\ \exp\left(\frac{(\gamma_{\mathrm{F}} - \gamma_{\mathrm{O}})y - (\gamma_{\mathrm{F}} + \gamma_{\mathrm{O}})|y|}{4}\right).$$

Using (15), S_{L0} can be written as

$$S_{\mathrm{L0}} = \sqrt{1 + \frac{(S+1)^2}{4S}|y|}\ \exp\left(\frac{(S^2-1)y - (S+1)^2|y|}{8S}\right), \tag{45}$$

in terms of the stoichiometric coefficient S. Thus, to leading order, the local burning speed is independent of the flow and depends only by S and the transverse coordinate y. For $S = 1$, for example, the above formula reduces to

$$S_{\mathrm{L0}} = \sqrt{1 + |y|}\exp\left(-\frac{|y|}{2}\right). \tag{46}$$

Figure 2 shows a plot of the burning speed S_{L0} for selected values of S. When $S = 1$, the burning speed is an even function of y with a peak located at the stoichiometric line $y = 0$. The peak is seen to move away from the stoichiometric line $y = 0$ towards the fuel side (right side) as S is increased. In all cases S_{L0} decays exponentially to zero for large value of $|y|$.

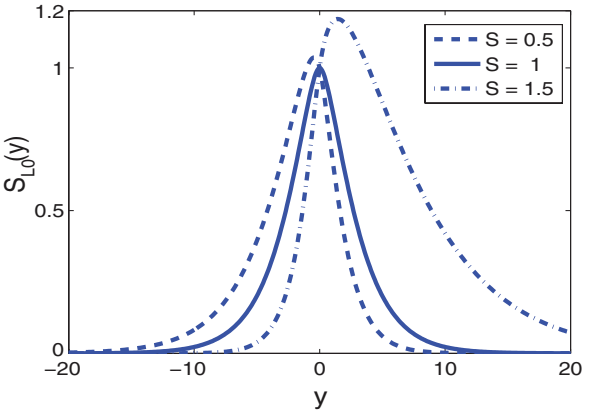

Figure 2. Leading order burning speed S_{L0} versus y for selected values of S.

4.4. *Flame speed and flame shape*

The first approximation to the flame speed V (with respect to the laboratory) given by 30 can now be determined to be

$$V_0 = S_{L0}(y^*) - u(y^*),$$

in which the leading edge(s) y^* will be found explicitly later once the flow has been specified. In the absence of flow, $u = 0$, $y^* = \bar{y}^*$ where $\bar{y}^*$ is the location of the maximum of $S_{L0}(y^*)$, given by

$$\bar{y}^* = \frac{S-1}{S+1}\left(1 + \frac{|S-1|}{S+1}\right). \tag{47}$$

Similarly, the propagation speed U (with respect to the gas at the leading edge) defined in (32) can be determined to be to leading order given by

$$U_0 = S_{L0}(y^*).$$

With V_0 being known, equations (34) and (45) can be reused to determine $f_0'(y)$ and hence, by integration, the flame shape to leading order $f_0(y)$. Thus, we obtain

$$f_0'^2 = \left(\frac{S_{L0}(y^*) + u(y) - u(y^*)}{S_{L0}(y)}\right)^2 - 1, \tag{48}$$

which specifies the combined effect of concentration inhomogeneities (non-constant $S_{L0}(y)$) and the flow $u(y)$ on the flame slope. Finally, the curvature of the flame-front at the leading edge $f_0''(y^*)$ can be evaluated by differentiating Equation (48), or using the second equality in (31), to obtain

$$f_0''(y^*) = \sqrt{\frac{u''(y^*) - S_{L0}''(y^*)}{S_{L0}(y^*)}}, \tag{49}$$

whose sign is consistent with (28). This formula clearly shows the dependence of the curvature at the leading edge on the flow field and the burning speed.

4.5. *The solution in the next approximation*

The above analysis provides a leading order description of the flame. For a better description, we carry out the asymptotic analysis to the next order in ϵ. The governing equations in the inner region are

$$(V_0+u(y))\frac{\partial\theta_1}{\partial\zeta}+V_1\frac{\partial\theta_0}{\partial\zeta}=\mathcal{F}(\theta_0)+\left(1+f_0'^2\right)\frac{\partial^2\theta_1}{\partial\zeta^2} \tag{50}$$

$$(V_0+u(y))\frac{\partial h_1}{\partial\zeta}+V_1\frac{\partial(h_0+l_{\mathrm{F}}\theta_0)}{\partial\zeta}=\mathcal{F}(h_0)+\left(1+f_0'^2\right)\frac{\partial^2(h_1+l_{\mathrm{F}}\theta_1)}{\partial\zeta^2}$$

$$(V_0+u(y))\frac{\partial k_1}{\partial\zeta}+V_1\frac{\partial(k_0+l_{\mathrm{O}}\theta_0)}{\partial\zeta}=\mathcal{F}(k_0)+\left(1+f_0'^2\right)\frac{\partial^2(k_1+l_{\mathrm{O}}\theta_1)}{\partial\zeta^2},$$

where

$$\mathcal{F}=2f_0'f_1'\frac{\partial^2}{\partial\zeta^2}-f_0''\frac{\partial}{\partial\zeta}-2f_0'\frac{\partial}{\partial\zeta\,\partial y}.$$

The jump conditions (26a–26c) at $\zeta=0$ give to $\mathcal{O}(\epsilon)$

$$[\theta_1]=[h_1]=[k_1]=0, \tag{51a}$$

$$\left[\frac{\partial h_1}{\partial\zeta}\right]=-l_{\mathrm{F}}\left[\frac{\partial\theta_1}{\partial\zeta}\right],\qquad\left[\frac{\partial k_1}{\partial\zeta}\right]=-l_{\mathrm{O}}\left[\frac{\partial\theta_1}{\partial\zeta}\right], \tag{51b}$$

$$\left[\frac{\partial\theta_1}{\partial\zeta}\right]=\left(\frac{\sigma_1}{2}+\frac{(h_1-k_1)(h_0-k_0)}{2(h_0-k_0)^2+4|h_0-k_0|}-\frac{f_0'f_1'}{1+f_0'^2}\right)\left[\frac{\partial\theta_0}{\partial\zeta}\right], \tag{51c}$$

where

$$\sigma_1=\frac{h_1+k_1}{2}-\frac{(h_1-k_1)(h_0-k_0)}{2|h_0-k_0|}.$$

Downstream of the reaction sheet, it is found that θ_1 must be zero so as to be bounded as $\zeta\to\infty$ and to allow matching with the outer solution. We thus have from (50) after eliminating exponentially growing terms

$$\theta_1=0,\quad h_1=\tilde{h}_1,\quad k_1=\tilde{k}_1\qquad\text{for}\quad\zeta\geq0, \tag{52}$$

where $\tilde{h}_1$ and $\tilde{k}_1$ are independent of ζ and are as yet undetermined.

We now integrate Equations (50) from $\zeta=-\infty$ to $\zeta=0^-$ to obtain

$$\left(1+f_0'^2\right)\left[\frac{\partial\theta_1}{\partial\zeta}\right]=I_\theta-V_1$$

$$(V_0+u(y))\tilde{h}_1=I_h+l_{\mathrm{F}}I_\theta \tag{53}$$

$$(V_0 + u(y))\tilde{k}_1 = I_k + l_{\rm O} I_\theta \,,$$

after using the jump conditions (52), the matching requirement that θ_1, h_1 and k_1 and their derivatives with respect to ζ must vanish as $\zeta \to -\infty$, and the fact that these derivatives must also vanish at $\zeta = 0^+$ on account of (52). In (53) we have introduced the quantities

$$I_\theta \equiv \int_{-\infty}^{0} \mathcal{F}(\theta_0) d\zeta, \quad I_h = \int_{-\infty}^{0} \mathcal{F}(h_0) d\zeta, \qquad \text{and} \quad I_k = \int_{-\infty}^{0} \mathcal{L}(k_0) d\zeta$$

which can be evaluated from (42–44) to yield

$$I_\theta = 2\lambda f_0' f_1' - f_0'' \,, \quad I_h = -2 l_{\rm F} \lambda f_0' f_1' \,, \quad I_k = -2 l_{\rm O} \lambda f_0' f_1' \,,$$

where λ is given by (41). Hence, we have

$$\begin{aligned} \left(1 + f_0'^2\right) \left[\frac{\partial \theta_1}{\partial \zeta}\right] &= 2\lambda f_0' f_1' - f_0'' - V_1 \\ (V_0 + u(y))\tilde{h}_1 &= -l_{\rm F} f_0'' \\ (V_0 + u(y))\tilde{k}_1 &= -l_{\rm O} f_0'' \,, \end{aligned} \tag{54}$$

in which $[\partial\theta_1/\partial\zeta]$ can be eliminated using (51c); thus (54) appears as a system of three equations for the four unknowns f_1', V_1, $\tilde{h}_1$ and $\tilde{k}_1$. Using this system of equations at the leading edge $y = y^*$, the unknown f_1' drops because $f_0'(y^*) = 0$, allowing V_1 to be determined by

$$V_1 = -\mathcal{L}(y^*) f_0''(y^*) \,,$$

where

$$\mathcal{L}(y) = 1 + \frac{l_{\rm F} + l_{\rm O}}{2} - \frac{l_{\rm F} - l_{\rm O}}{2} \frac{(S+1)^2 y}{4S + (S+1)^2 |y|} \,. \tag{55}$$

Thus, a two-term approximation to the flame speed V is now available and is given by

$$V \sim S_{\rm L0}(y^*) - u(y^*) - \epsilon \mathcal{L}(y^*) f_0''(y^*), \tag{56}$$

which shows the dependence of V on the Lewis numbers and on the local burning velocity, the flow, and the flame curvature at the leading edge. In this formula, which is one of the main aims of the analysis, all terms are readily available; indeed $S_{\rm L0}(y^*)$, y^*, $f_0''(y^*)$, and $\mathcal{L}(y^*)$ are to be determined from (45), (29), (49), and (55).[2]

Finally, with V_1 determined, we can reuse the system of equations (54) for values of y different from y^* to find f_1', $\tilde{h}_1$ and $\tilde{k}_1$. The results can be used, in particular, to find the

[2]Strictly speaking, y^* should be denoted by y_0^* since it stands for the leading-order location of the leading edge. It is to be determined precisely as the location of a global maximum of $S_{\rm L0} - u$. Since we only need a leading-order approximation to y^*, we will not use any additional subscript.

perturbation in the burning velocity S_{L1} introduced in (35). Then, from Equation (33), we find that S_L can be expressed in the form

$$S_L \sim S_{L0}(y)[1 - \mathcal{L}(y)\kappa(y)], \tag{57}$$

where $\mathcal{L}(y)$ and $\kappa(y)$ appear as a *local Markstein length* and a *local flame stretch*, respectively, the latter being found to be given by

$$\kappa(y) = \frac{\epsilon}{S_{L0}(y)} \frac{f_0''(y)}{\sqrt{1 + f_0'^2(y)}}.$$

We have now completed our asymptotic analysis of triple-flame propagation in a parallel flow. Explicit analytical formulae describing the shape, the propagation speed and the local burning velocity of the flame-front have been obtained. These formulae involve the leading edge of the flame-front, y^*, which can be determined from Equation (29), or more precisely as the location of a global maximum of $S_{L0}(y) - u(y)$. To further qualify the flame behaviour, we need to specify the flow. In the next section, we shall consider the case of a Poiseuille flow (in a porous channel); in this case the flow-scale, which is determined by the channel width, is large compared to the flame-front radius of curvature. Then, in Section 6, we shall consider a flow, more specifically a harmonic flow, whose scale is equal in order of magnitude to the flame-front radius of curvature.

5. Application to Poiseuille flow in a porous channel

We study in this section triple-flame propagation in the presence of a parallel flow whose scale is large compared to the flame radius of curvature L/β. Specifically, we consider the case of a Poiseuille flow in a porous channel of width L given, in terms of dimensional quantities, by

$$\tilde{u} = \tilde{A}\left(1 - \frac{Y^2}{L^2}\right).$$

In non-dimensional form we have

$$u = A\left(1 - \left\{\frac{1-S}{1+S} + \frac{y}{\beta}\right\}^2\right),$$

where $u = \tilde{u}/S_L^0$, $A = \tilde{A}/S_L^0$, and $y = \beta(Y - Y_{st})/L$, after using (6). We note that

$$u \sim \frac{4S}{(1+S)^2} A \tag{58}$$

in the limit $\beta \to \infty$, in the flame-front region $y \sim 1$. Thus the flow appears as uniform, with an effective amplitude depending on the stoichiometric coefficient S. On using (58) in the analytical results derived above, a description of the flame-front is readily obtained. Indeed the uniformity of the flow for $y \sim 1$ implies that the location of the leading edge y^* corresponds simply to the maximum of $S_L(y)$, as dictated by (29), and is thus independent

of the flow. Using (29), (45), and (49), we thus find

$$y^* = \frac{S-1}{(S+1)}\left(1+\frac{|S-1|}{S+1}\right), \tag{59}$$

$$S_{\mathrm{L}0}(y^*) = \frac{\sqrt{2(S+1)}}{S+1-|S-1|}\exp\left(-\frac{1}{2}\frac{|S-1|}{S+1}\right), \tag{60}$$

and

$$f_0''(y^*) = \frac{S+1}{(S+1+|S-1|)\sqrt{2}}, \tag{61}$$

which are, respectively, the leading order approximation for the location of the leading edge, and for the burning velocity and curvature of the flame-front there. Furthermore, on using (59) in (55) we find

$$\mathcal{L}(y^*) = 1 + \frac{l_{\mathrm{F}}}{S+1} + \frac{S\,l_{\mathrm{O}}}{S+1}. \tag{62}$$

A fully explicit two-term approximation of the flame speed V is now available using (56) and (58), namely,

$$V \sim S_{\mathrm{L}0}(y^*) - \frac{4S}{(1+S)^2}\,A - \left(1+\frac{l_{\mathrm{F}}}{S+1}+\frac{S\,l_{\mathrm{O}}}{S+1}\right)\epsilon f_0''(y^*), \tag{63}$$

with $S_{\mathrm{L}0}(y^*)$ and $f_0''(y^*)$ given by (60) and (61). The propagation speed $U \equiv V + u(y^*)$ introduced in (32) consequently satisfies

$$U \sim S_{\mathrm{L}0}(y^*) - \left(1+\frac{l_{\mathrm{F}}}{S+1}+\frac{S\,l_{\mathrm{O}}}{S+1}\right)\epsilon f_0''(y^*), \tag{64}$$

on taking 58 into account.

We conclude that the presence of the large-scale Poiseuille flow only modifies the flame speed V through the second term on the right-hand side of 63 but has no influence on the propagation speed U, the local burning speed $S_{\mathrm{L}}(y)$ and the flame shape $f(y)$. Similar behaviour is of course expected for flames propagating in parallel flows whose transverse length-scale is of the order of the mixing layer thickness, since these appear uniform on the transverse length-scale of the flame-front.

We close this section by illustrating the results in the special case $S = 1$ for which we obtain $y^* = 0$,

$$U \sim 1 - \left(1+\frac{l_{\mathrm{F}}}{2}+\frac{l_{\mathrm{O}}}{2}\right)\frac{\epsilon}{\sqrt{2}},$$

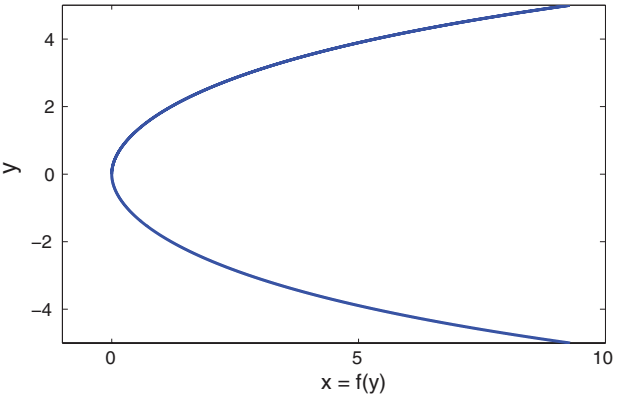

Figure 3. Shape of the flame-front $f_0(y)$ for $S = 1$.

$V = U + A$ and $S_{L0}(y)$ as given by 46. Equation 48 then implies that $f_0' = \mathrm{sgn}(y)(S_{L0}^{-2}(y) - 1)^{1/2}$, and hence, by numerical integration (using the condition $f_0(0) = 0$), that the shape of the flame-front $f_0(y)$ is as depicted in Figure 3.

6. Application to a harmonic flow

We consider in this section triple-flame propagation in a parallel flow whose scale is of the order of magnitude of the flame-front radius of curvature (L/β). To illustrate the methodology, we specifically consider the case of a harmonic flow given in non-dimensional form by

$$u(y) = A\cos(\pi y), \tag{65}$$

where A is the flow intensity (measured with S_L^0) and y the transverse coordinate (measured with L/β).

A two-term approximation to the flame speed V (relative to the laboratory) in this case is obtained on using 65 in 56:

$$V \sim S_{L0}(y^*) - A\cos(\pi y^*) - \epsilon\left(1 + \frac{l_F + l_O}{2} - \frac{l_F - l_O}{2}\frac{(S+1)^2 y^*}{4S + (S+1)^2|y^*|}\right) f_0''(y^*), \tag{66}$$

in which $S_{L0}(y^*)$ and $f_0''(y^*)$ are given by (45) and (29). The main task is thus to determine the leading edge location y^*, and to this end we shall use the simple criterion of Section 3.2, namely that y^* must be a global maximum of the function $S_{L0}(y) - u(y)$.

The symmetrical case $S = 1$

We begin with the stoichiometrically symmetrical case $S = 1$, for which S_{L0} is given by (45). A necessary condition for y^* to be a maximum of $S_{L0}(y) - u(y)$ is thus that it satisfies the equation

$$-\frac{y e^{-|y|/2}}{2\sqrt{1+|y|}} + A\pi\sin(\pi y) = 0\,, \tag{67}$$

for which $y = 0$ is a root for any value of A. An elementary study shows that this trivial root corresponds to a unique global maximum if $A < A_c \approx 0.0451$, a non-global maximum for $A_c < A < 1/2\pi^2$ and a minimum for $1/2\pi^2 < A$. For $A > A_c$, we have two global maxima symmetrically located with respect to the origin. We conclude that the flame-front must have two leading edges which are symmetrically located with respect to the stoichiometric line $y = 0$ when $A > A_c$, while a single leading edge located at $y = 0$ is expected for $A < A_c$ (including negative values of A).

The results to leading order are summarized in Figure 4, which shows the location of the leading edge y^* (top), the propagation speed $U \sim S_{\mathrm{L0}}(y^*)$ (middle), and the flame speed $V \sim S_{\mathrm{L0}}(y^*) - u(y^*)$ (bottom), versus the flow amplitude A. We note that to the jump in y^* at $A = A_c$ observed (from $y = 0$ to $y = \pm y_c \approx \pm 0.3475$), there corresponds a jump in the leading-order propagation speed U (from $U = 1$ to $U \approx 0.975$); however the flame speed V remains continuous because the function $S_{\mathrm{L0}} - u$ has three global maxima when $A = A_c$, located at $y = 0$ and $y = \pm y_c$, such that $S_{\mathrm{L0}}(\pm y_c) - u(\pm y_c) = S_{\mathrm{L0}}(0) - u(0) = V$.

It is interesting to note that V exhibits a non-monotonic dependence on A, which is intimately linked to behaviour of y^*. Indeed, the linear decrease of V is due to the fact that for $A < A_c$ we have $y^* = 0$ and hence $V \sim S_{\mathrm{L0}}(0) - u(0) = 1 - A$. As A increases above A_c, however, y^* moves away from the origin leading to an exponential decrease in $S_{\mathrm{L0}}(y^*)$ according to 45 which is dominated by an algebraic increase in $-u(y^*)$ (for $|y^*| < 1$) so that $V \sim S_{\mathrm{L0}}(y^*) - u(y^*)$ is an increasing function of y^* and hence of A. As A increases the global maxima of $S_{\mathrm{L0}}(y) - u(y)$ tend to $(\pm 1, -u(\pm 1))$ which are the global maxima of $-u(y)$ closest to $y = 0$; this determines the asymptotic behaviour $y^* \sim \pm 1$ and $V \sim S_{\mathrm{L0}}(\pm 1) + A = \sqrt{2/e} + A$ for $A \gg 1$; in fact for these asymptotic values to be good approximations for y^* and V, A needs only to be moderately large, say $A > 1$.

Finally, to complete the leading-order description of the flame we plot in Figure 6 $f_0(y)$ for selected values of A and $S = 1$, based on a numerical solution of 48. The figure illustrates how the flow deforms the flame, and shifts its leading edge towards $y = \pm 1$ for $A > 0$ (except for very small values of $A < A_c \approx 0.0451$ which are not shown). For $A < 0$, the flame has a single edge. In all cases, an increase in $|A|$ is seen to typically decrease the transverse extent of the flame-front and to increase its curvature at the leading-edge(s). To account for curvature effects, we now turn to the two-term approximation of V given in 66, which we plot versus A in Figure 5 for selected values of ϵ in the case where $l_{\mathrm{F}} = l_{\mathrm{O}} = 0$. We note that all curves present a slope discontinuity at $A = A_c$, and more importantly that account of curvature effects decreases the value of V by an amount which increases with the magnitude of the flow amplitude, $|A|$. More specifically, fully explicit expressions for V can be written down using 45 and the determination of y^* discussed above. We find that

$$V \sim 1 - A - \frac{\epsilon}{\sqrt{2}}\sqrt{1 - 2\pi^2 A} \qquad \text{for} \quad A < A_c\,, \tag{68}$$

including negative values of A, and that

$$V \sim \sqrt{\frac{2}{e}} + A - \epsilon \left(\frac{e}{2}\right)^{1/4} \pi \sqrt{A} \qquad \text{for} \quad A > 1\,, \tag{69}$$

or strictly speaking for $A \gg 1$. The formulae show that V depends linearly on A in the first approximation (i.e for $\epsilon = 0$) with correction proportional to ϵ multiplied by $\sqrt{|A|}$ for $|A|$ sufficiently large (but such that $\epsilon\sqrt{|A|} \ll 1$ for the ϵ-expansion to make sense).

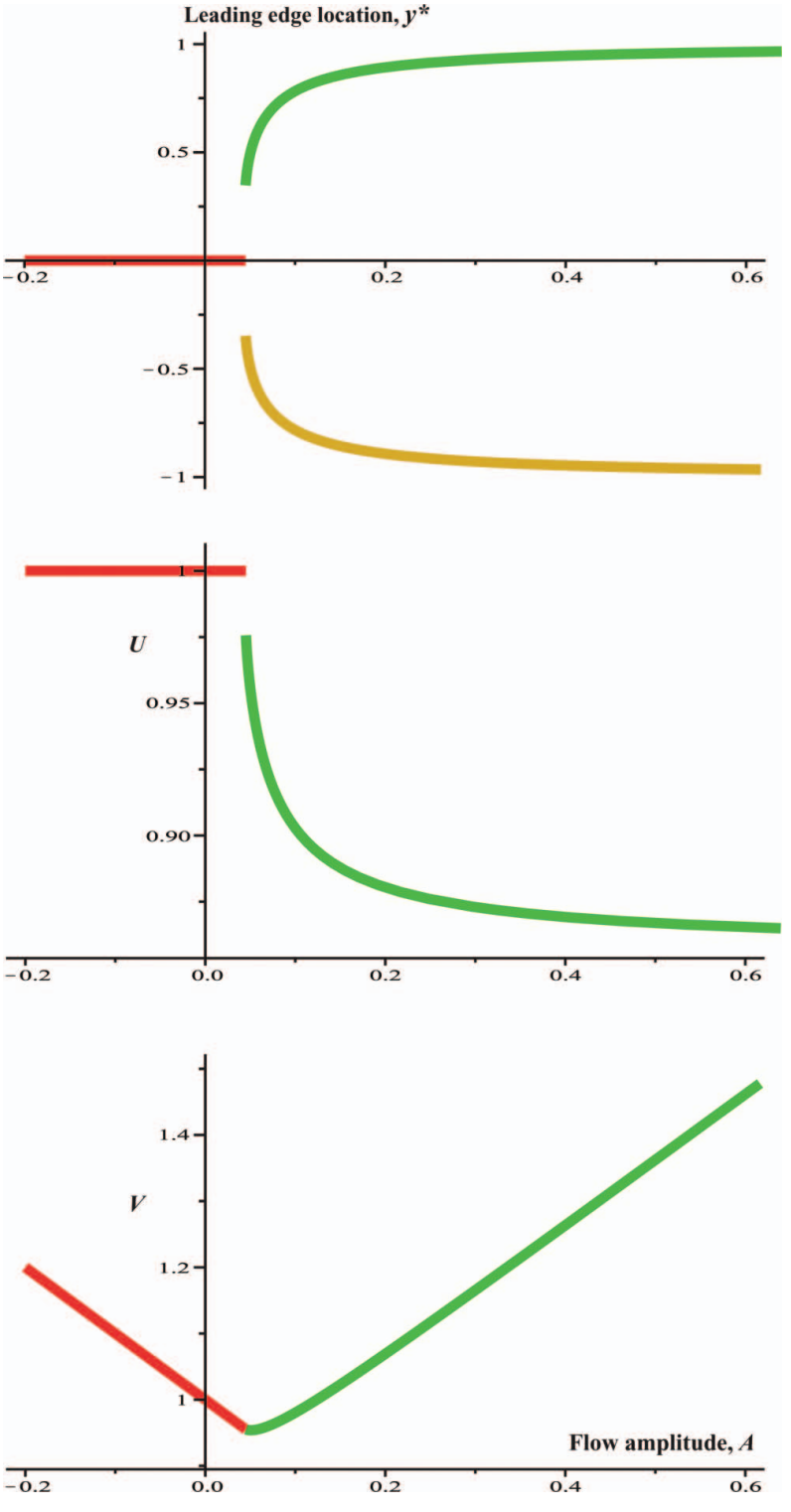

Figure 4. Leading edge location y^* (top), propagation speed U (middle), and flame speed V (bottom) versus the flow amplitude A, to leading order.

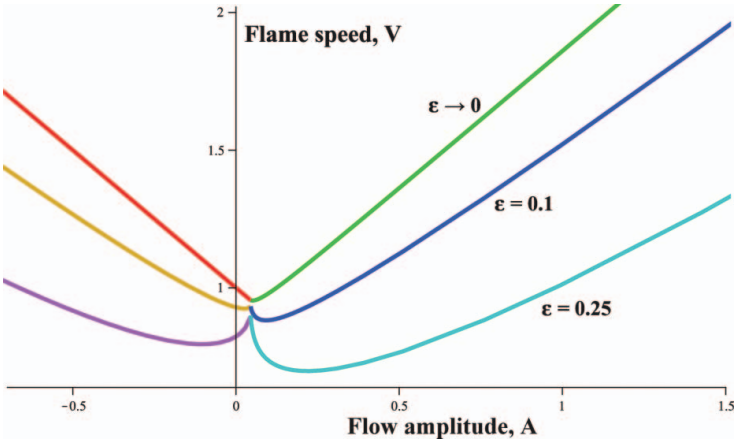

Figure 5. Flame speed V versus the flow amplitude A based on the two-term approximation (66) for selected values of ϵ, $S = 1$, and $l_F = l_O = 0$.

Results for a non-unit value of S

The results just presented were obtained for a flame which is symmetrical with respect to the stoichiometric line $y = 0$ given our choice $S = 1$ and the symmetry of the flow 65 (and equal Lewis numbers). We now consider a case with non-unit value of S, namely $S = 2$, where this symmetry is broken. Again, a key step is the determination of the leading edge as a global maximum of $S_{L0} - u$, where S_{L0} is given by (45) with $S = 2$. An elementary study shows that $S_{L0} - u$ has a unique global maximum for any value of A and that the

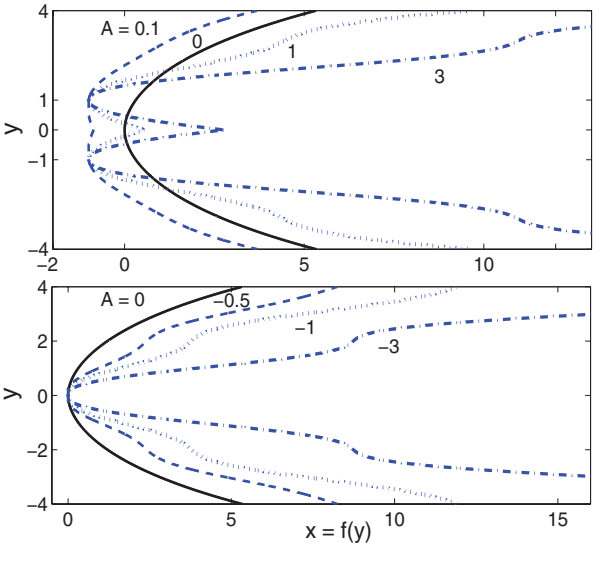

Figure 6. Flame shape $f_0(y)$ for selected values of A and $S = 1$.

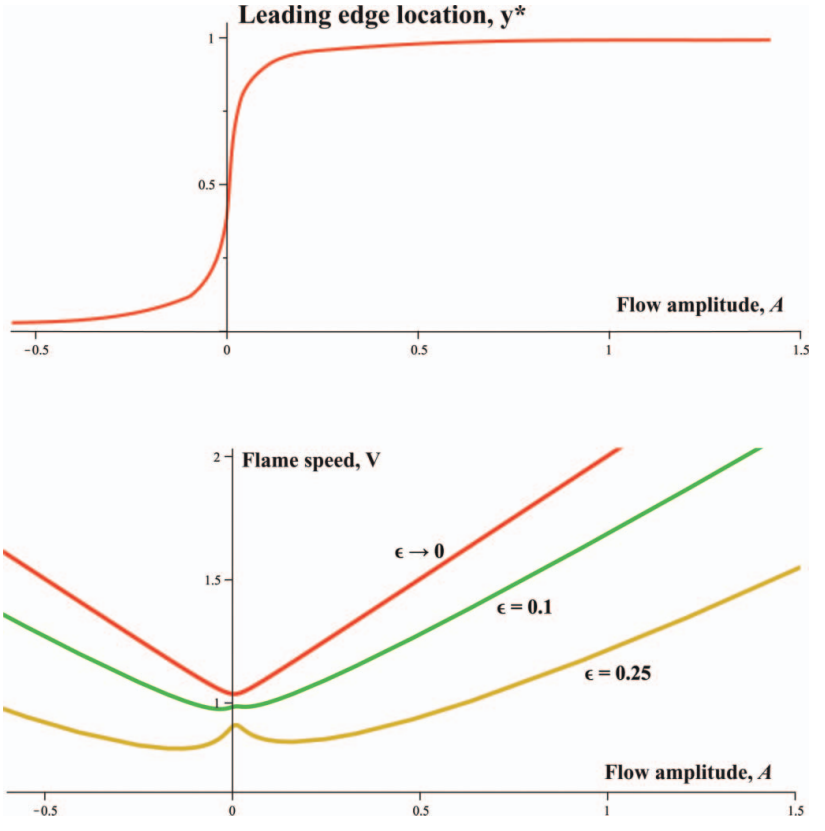

Figure 7. Leading edge location y^* versus A (top) and flame speed V (based on the two-term approximation (66)) versus A for selected values of ϵ (bottom); $S = 2$ and $l_F = l_O = 0$.

location y^* of this maximum satisfies $0 < y^* < 1$ and is related to A by the explicit relation

$$A = \frac{3\,(9y^* - 4)\,\exp(-3y^*/8)}{16\,\pi\,\sqrt{18y^* + 16}\,\sin(\pi\,y^*)}\,. \tag{70}$$

With y^* thus determined, we may now use the two-term expansion (56) for the flame speed V. The results are summarized in Figure 7 showing y^* versus A (top), and V versus A for selected values of ϵ and $l_F = l_O = 0$ (bottom). We note that, unlike in the case $S = 1$, the leading edge y^* is now a function of A which is continuous, in addition to being single-valued. Furthermore we record the asymptotic behaviour $y^* \to 1$ as $A \to \infty$ and $y^* \to 0$ as $A \to -\infty$, with the asymptotic values being in fact closely approached by y^* for values of A of order unity. The asymptotic behaviour is simply explained by noting that $y = 1$ (respectively $y = 0$) is the location of the maximum of $-u(y)$ which is closest to $\bar{y}^*$ when $A > 0$ (respectively $A < 0$); here $\bar{y}^* = 4/9$ is the location of the leading edge in the absence of flow, $A = 0$, as given by 47. Turning to the flame speed V, we note that a non-monotonic dependence on A may be obtained for non-zero values of ϵ, both for $A > 0$

and $A < 0$. For large, or moderately large, values of $|A|$, it can be shown that

$$V \sim \left(\frac{17}{8}e^{-3/4}\right)^{1/2} + A - \epsilon\left(\frac{17}{8}e^{-3/4}\right)^{-1/4}\pi\sqrt{A}\,,$$

if A is positive, and

$$V \sim 1 - A - \epsilon\pi\sqrt{-A}\,, \tag{71}$$

if $A < 0$. Thus, as in the case $S = 1$, V depends linearly on A in the first approximation (i.e for $\epsilon = 0$) with correction proportional to ϵ multiplied by $\sqrt{|A|}$ for $|A|$ sufficiently large.

Generalization and additional results

To test the influence of varying the flow-scale, we slightly generalize the flow given in (65) to become

$$u = A\cos\frac{\pi y}{\ell}\,,$$

where ℓ is the (non-dimensional) flow-scale. Again, the location y^* of the leading edge is to be determined as a global maximum of $S_{\mathrm{L0}} - u$, and a necessary condition for this is that y^* satisfies

$$A = \frac{\ell(S+1)^3}{8\pi S(S+1+|S-1|)}\,\frac{(y^*-\bar{y}^*)}{\sin(\frac{\pi y^*}{\ell})}\,\frac{\exp\left(\dfrac{(S^2-1)y^* - (S+1)^2|y^*|}{8S}\right)}{\sqrt{1+\dfrac{(S+1)^2}{4S}|y^*|}}, \tag{72}$$

where $\bar{y}^*$ is the location of the leading edge in the absence of flow given by (47). Clearly, Equation (72) reduces for $\ell = 1$ to (67) when $S = 1$ and to (70) when $S = 2$, as it should. More importantly, we note that the right-hand side of (72) is only defined for y^* belonging to open intervals of the form $(n\ell, (n+1)\ell)$, where n is an arbitrary integer. There is typically, however, a unique such interval which has physical significance, namely the one containing $\bar{y}^*$; this interval is given by $(y^*_{\min}, y^*_{\max}) \equiv (n\ell, (n+1)\ell)$, where $n = \mathrm{floor}(\bar{y}^*/\ell)$, with $\mathrm{floor}(x)$ designating the largest integer which is less or equal to x. This is so, except if $\bar{y}^*/\ell$ is an integer. For example, for $S > 1$, for which $\bar{y}^* > 0$ on account of 47, we have $n = 0$ for $\ell > \bar{y}^*$, $n = 1$ for $\bar{y}^*/2 < \ell < \bar{y}^*$, and more generally $n = k$ for $\bar{y}^*/(k+1) < \ell < \bar{y}^*/k$, for any positive integer k. Thus,

$$(y^*_{\min}, y^*_{\max}) = \begin{cases} (0, \ell) & \text{for} \quad \ell > \bar{y}^* \\ (n\ell, (n+1)\ell) & \text{for} \quad \dfrac{\bar{y}^*}{n+1} < \ell < \dfrac{\bar{y}^*}{n} \end{cases} \qquad (S > 1)\,. \tag{73}$$

In the special cases where $\bar{y}^*/\ell$ is an integer, equal to n, $(y^*_{\min}, y^*_{\max})$ must be taken to be $((n-1)\ell, (n+1)\ell)$. For example, such special cases occur for all values of ℓ when $S = 1$, since then $\bar{y}^*/\ell$ is equal to zero on account of 47 and hence $(y^*_{\min}, y^*_{\max}) = (-\ell, \ell)$, as seen in Figure 4 pertaining to $\ell = 1$.

In all cases, by letting y^* sweep the interval $(y^*_{\min}, y^*_{\max})$, A versus y^*, and thus y^* versus A, can be generated using Equation (72), although special care must be exercised in cases

where (72) specifies y^* as a multi-valued function of A. In turn, knowledge of y^* allows determination of V and U, using (56) and (32), and the dependence on ℓ may be written down explicitly, at least for large values of $|A|$.

Thus, for $S > 1$ and large negative values of A, we find that

$$U \sim V + A \sim 1 - \frac{\epsilon\pi}{\ell}\sqrt{-A}\,, \tag{74}$$

assuming that the flow-scale $\ell > \bar{y}^*$ and using (73) along with the fact that

$$y^* \to 0\,,\ u(y^*) \to A\,,\ u''(y^*) \to -\frac{A\pi^2}{\ell^2} \quad \text{as} \quad A \to -\infty\,.$$

Equation (74) generalizes (71) and indicates that U is independent of ℓ, equal to one, to leading order. It also shows that the curvature term decreases in inverse proportion to increasing ℓ, and the formula exhibits a remarkable independence of the stoichiometric coefficient S, in the limit considered. This independence of S and the simple dependence on ℓ are not encountered for large positive values of A, for which we obtain

$$U \sim V - A \sim S_{\mathrm{L}0}(\ell) - \frac{\epsilon\pi}{\ell}\sqrt{\frac{A}{S_{\mathrm{L}0}(\ell)}}\,, \tag{75}$$

again using (73) and the fact that

$$y^* \to \ell\,,\ u(y^*) \to -A\,,\ u''(y^*) \to \frac{A\pi^2}{\ell^2} \quad \text{as} \quad A \to +\infty\,.$$

Equation (75) exhibits an essentially exponential decrease of U with ℓ, to leading order, on account of (45). Interestingly, it also indicates that the curvature term, proportional to $\ell^{-1}S_{\mathrm{L}0}^{-1/2}(\ell)$, is a non-monotonic function of ℓ.

We now examine the effect of small-scale flow, $\ell \ll 1$, with $\epsilon \ll \ell$ however. In this case, (73) implies that the width of the interval $(y^*_{\min}, y^*_{\max})$ sandwiching $\bar{y}^*$, equal to ℓ, is also $\ll 1$; that is the small-scale flow negligibly affects the location of the leading edge y^*. We thus find that

$$U \sim V \mp A \sim S_{\mathrm{L}0}(\bar{y}^*) - \frac{\epsilon\pi}{\ell}\sqrt{\frac{|A|}{S_{\mathrm{L}0}(\bar{y}^*)}} \quad \text{as} \quad A \to \pm\infty\,. \tag{76}$$

This equation shows that U is equal to the propagation speed of the triple-flame in the absence of flow, to leading order, and that the curvature term[3] is inversely proportional to ℓ.

At this point, we note that the results just derived for $S > 1$ provide readily similar results for $0 < S < 1$, given that a change of S to S^{-1} merely changes y^* to its negative and the graphs of $S_{\mathrm{L}}(y)$ and $f(y)$ to their symmetric with respect to the $y = 0$ axis, without affecting U or V. Thus, 76 is still applicable if $S < 1$, and so are 74 and 75 provided that

[3]For this ϵ-expansion to make sense, we further assume that $\epsilon|A|^{1/2}/\ell \ll 1$.

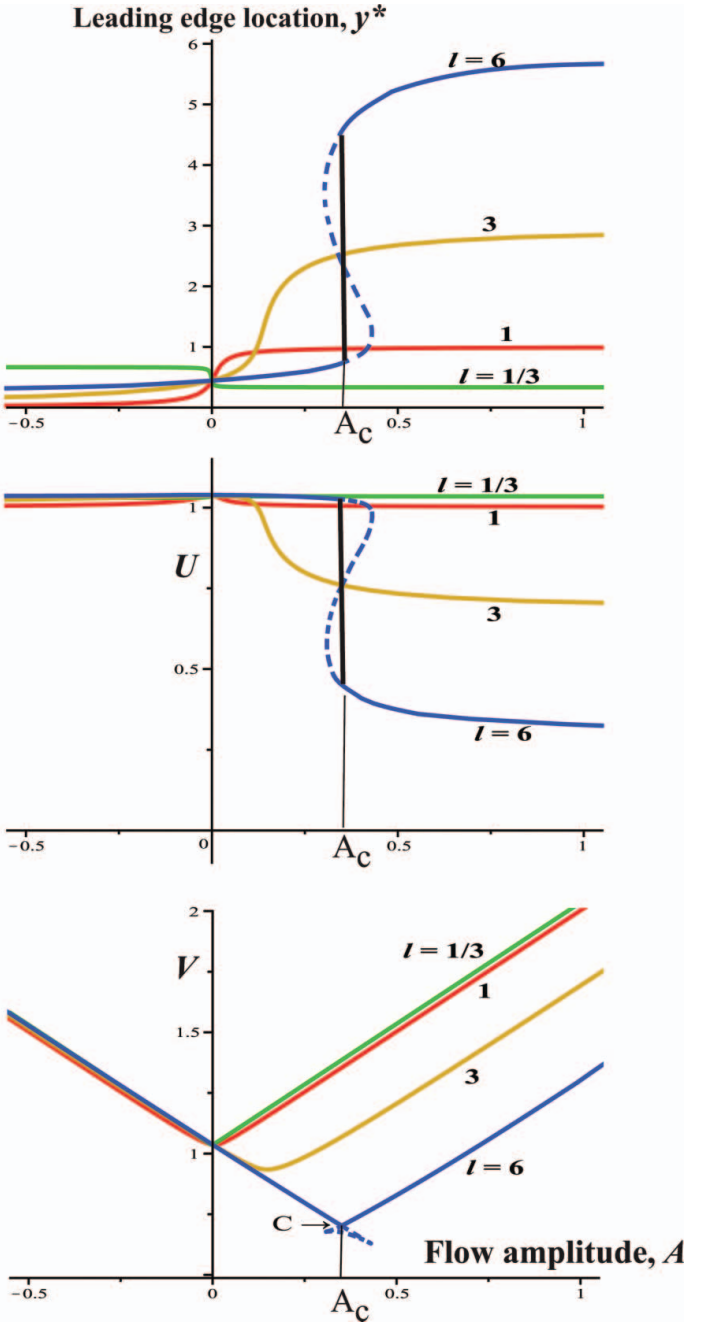

Figure 8. Leading edge location y^* (top), propagation speed U (middle), and flame speed V (bottom) versus the flow amplitude A for selected values of ℓ, to leading order ($\epsilon = 0$). The dashed portions of the curves corresponding to $\ell = 6$ are to be discarded.

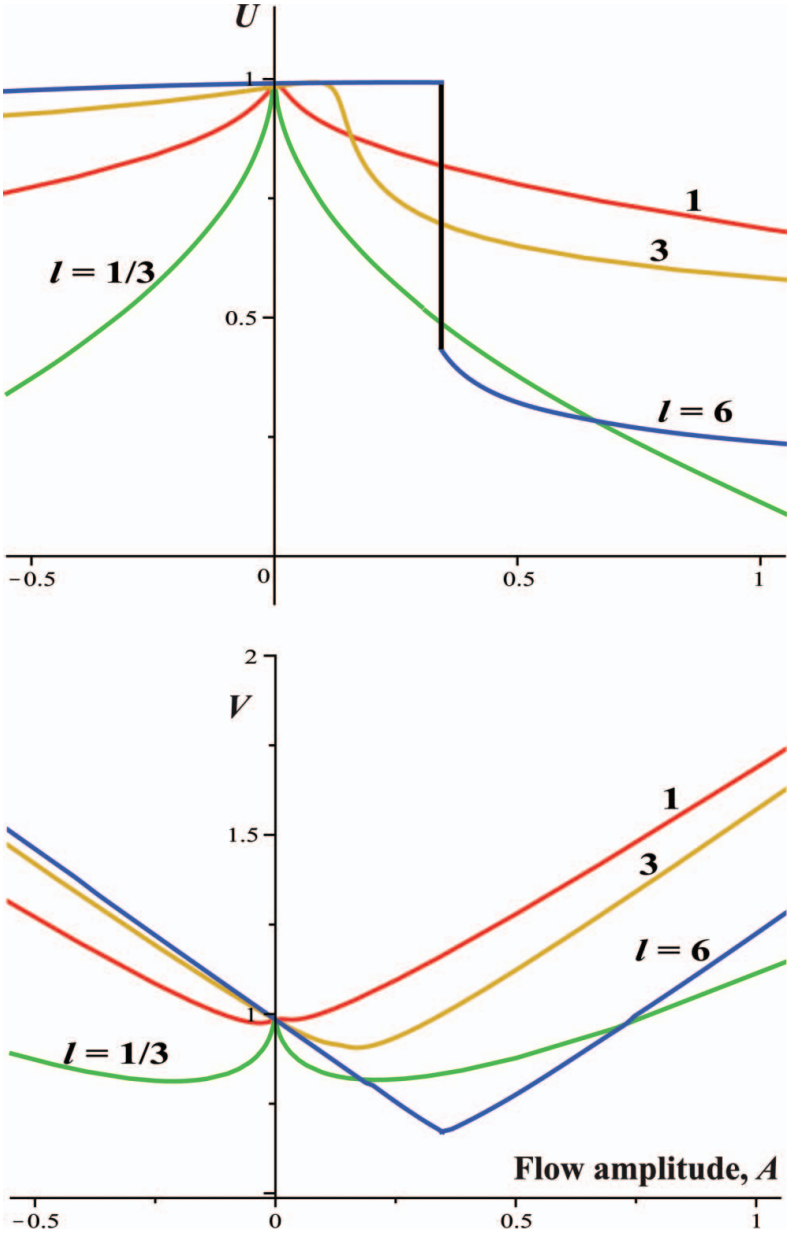

Figure 9. Propagation speed U and flame speed V versus A for selected values of ℓ and $\epsilon = 0.1$.

$\ell > |\bar{y}^*|$ and that $S_{L0}(\ell)$ is replaced by $S_{L0}(-\ell)$. As for the symmetrical case $S = 1$, a study similar to that carried out leading to Figures 4 and 5 reveal, in particular, that

$$U \sim V + A \sim 1 - \epsilon\sqrt{\frac{1}{2} - \frac{A\pi^2}{\ell^2}} \qquad \text{for} \quad A \leq 0\,, \tag{77}$$

and

$$U \sim V - A \sim S_{\mathrm{L}0}(\ell) - \frac{\epsilon\pi}{\ell}\sqrt{\frac{A}{S_{\mathrm{L}0}(\ell)}} \qquad \text{for} \quad A \gg 1\,. \tag{78}$$

Clearly, (77) generalizes (68) to arbitrary values of ℓ, and vividly illustrates the influence of the flow for negative or zero values of A. Similarly, (78) generalizes (69), and exhibits a curvature term, proportional to $\ell^{-1} S_{\mathrm{L}0}^{-1/2}(\ell)$, which is a non-monotonic function of ℓ.

As a final example, we reconsider the case $S = 2$, described in Figure 7 for $\ell = 1$, which we reexamine for selected values of ℓ. Shown in Figure 8 are the leading-order results representing y^* (top), $U \sim S_{\mathrm{L}0}(y^*)$ (middle), and $V \sim S_{\mathrm{L}0}(y^*) - u(y^*)$ (bottom), versus the flow amplitude A. We note that the figure is generated using 72, 56 and 32 with the intervals of variation of y^* selected to be (1/3, 2/3), (0, 1), (0, 3) and (0, 6), for $\ell = 1/3$, 1, 3, and 6, respectively, as dictated by 73.[4] An important feature observed in the figure is the multi-valued dependence on A when $\ell = 6$, which is in fact found for values of $\ell > 4.5$, approximately. The cases of multi-valued behaviour can be resolved by examining whether the values of y^* plotted are true global maxima of $S_{\mathrm{L}0} - u$, as discussed in connection with Figure 4. Graphically, we have observed that multi-valued behaviour occurs when the curve of V versus A crosses itself. This happens in the case $\ell = 6$ at the point C indicated in the bottom subfigure, corresponding to an amplitude A_c; the portion of the V-curve below this point must be discarded along with the dashed portions of the curves in the top and middle subfigures. A single value behaviour is thus obtained with a jump discontinuity for y^* and U, and a slope discontinuity for V, at $A = A_c$. Finally, with meaningless portions of curves similarly discarded, we plot in Figure 9 the curves representing U and V versus A for $\epsilon = 0.1$. We simply remark that Figures 8 and 9 both confirm and illustrate the asymptotic behaviours predicted by Equations (74–76), which have been discussed earlier.

7. Concluding remarks

We have presented an analytical study of triple-flame propagation against a parallel flow in a mixing layer, based on a thermo-diffusive model. The analysis has been carried out in the asymptotic limit of large Zeldovich number and small values of ϵ, where ϵ is a measure of the flame-front thickness relative to its typical radius of curvature. Analytical expressions describing the local burning velocity, the shape of the flame-front, and the overall flame speed have been derived. In particular, a two-term expansion of the latter for small ϵ has been given, Equation (56). Two cases have been considered to illustrate the influence of the flow on triple-flame propagation. In the first case, corresponding to a Poiseuille flow in a porous channel, the flow-scale is large compared to the flame-front radius of curvature and is thus found to negligibly affect the flame structure except for a change in its speed by an amount which depends on the stoichiometric conditions of the mixture. In the second case, the effects of harmonic flows whose scale is of the order of the flame radius of curvature have been studied; these were found to significantly wrinkle the flame-front, shift its leading edge away from the stoichiometric line, and modify its overall speed. The results presented

[4] It may be useful to point out that 72 and 73 imply that $y^* \to y^*_{\min}$ as $A \to -\infty$, $y^* \to y^*_{\max}$ as $A \to +\infty$ if $n \equiv \mathrm{floor}(\bar{y}^*/\ell)$ is even, and $y^* \to y^*_{\max}$ as $A \to -\infty$, $y^* \to y^*_{\min}$ as $A \to +\infty$ if n is odd. This explains why y^* is a decreasing function of A for $\ell = 1/3$, but not for the other values of ℓ considered.

describe, in particular, a systematic way of determining the leading-edge of the flame-front in terms of the flow amplitude A which is critical in determining the flame speed. The latter is found to depend linearly on A in the first approximation with correction proportional to the flame thickness multiplied by $\sqrt{|A|}$, for $|A|$ sufficiently large. Furthermore, in the context harmonic flows, the effect of varying the flow-scale on flame propagation has been investigated, with insightful formulae derived, and interesting behaviours such as non-monotonic dependence on the flow-scale identified.

The approach adopted and the results obtained constitute valuable tools to further investigate flame propagation in non-uniform reactive mixtures under more complex flows. However, even in the simple case of parallel flows considered, many important aspects remain to be studied since they are outside the scope of this asymptotic study. These include the effect of flows with small scales, of order ϵ or smaller, finite values of the Zeldovich number, and non-small values of ϵ leading to extinction fronts. These aspects necessitate a numerical approach and will be discussed in a separate study.

Acknowledgments

The authors would like to thank Dr. Guy Joulin and Prof. John Dold for helpful discussions and suggestions concerning this work.

References

[1] H. Phillips, Flame in a buoyant methane layer. *Tenth Symposium (International) on Combustion*, The Combustion Institute, 10 (1965), pp. 1277–1283.

[2] Y. Ohki and S. Tsuge, *Flame propagation through a layer with varying equivalence ratio*, in *Dynamics of Reactive Systems, Part 1: Flames and Configurations*, J. Leyer J. Bowen and R. Soloukhin, eds., Progress in Astronautics and Aeronautics, vol. 105, American Institute of Aeronautics and Astronautics, 1986, page 233.

[3] J. Dold, *Flame propagation in a nonuniform mixture: Analysis of a slowly varying triple-flame*, Combust. Flame, 76 (1989), pp. 71–88.

[4] J. Hartley and J. Dold, *Flame propagation in a nonuniform mixture: Analysis of a propagating triple-flame*, Combust. Theory Model., 80 (1991), pp. 23–46.

[5] S. Chung, *Stabilization, propagation and instability of tribrachial triple flames*, Proc. Combust. Inst., 31 (2007) pp. 877–892.

[6] J. Daou and A. Liñán, *The role of unequal diffusivities in ignition and extinction fronts in strained mixing layers*, Combust. Theory Model., 2 (1998), pp. 449–477.

[7] R. Daou, J. Daou, and J. Dold, *The effect of heat loss on flame edges in a non-premixed counterflow within a thermo-diffusive model*, Combust. Theory Model., 8 (2004), pp. 683–699,

[8] J. Daou, R. Daou, and J. Dold, *Effect of volumetric heat loss on triple-flame propagation*, Proc. Combust. Inst., 29 (2002), pp. 1559–1564.

[9] M.S. Cha and P.D. Ronney, *Propagation rates of non-premixed edge-flames*, Combust. Flame, 146 (2006), pp. 312–328.

[10] J. Daou and S. Ali, *Effect of the reversibility of the chemical reaction on triple flames*, Proc. Combust. Inst., 31 (2007), pp. 919–927.

[11] J. Daou, *Asymptotic analysis of flame propagation in weakly-strained mixing layers under a reversible chemical reaction*, Combust. Theory Model., 13 (2009), pp. 189–213.

[12] N. Kim, J. Seo, Y. Guahk, and H. Shin, *The propagation of tribrachial flames in a confined channel*, Combust. Flame, 146 (2006), pp. 168–179.

[13] P. Kioni, B. Rogg, K. Bray, and A. Liñán, *Flame spread in laminar mixing layers: The triple flame*, Combust. Flame, 95 (1993), pp. 277–290.

[14] J. D. Buckmaster and G. S. S. Ludford, *Lectures on Mathematical Combustion*, Society for Industrial and Applied Mathematics, Philadelphia, 1983.